Impact of physicality on network structure

Márton Pósfai [1,6], **Balázs Szegedy**[2,6], **Iva Bačić** [1,3], **Luka Blagojević** [1], **Miklós Abért**[2], **János Kertész** [1], **László Lovász**[2] & **Albert-László Barabási** [1,4,5] ✉

一、研究背景：为什么要关注"物理网络"？

The emergence of detailed maps of physical networks, such as the brain connectome, vascular networks or composite networks in metamaterials, whose nodes and links are physical entities, has demonstrated the limits of the current network science toolset. Link physicality imposes a non-crossing condition that affects both the evolution and the structure of a network, in a way that the adjacency matrix alone—the starting point of all graph-based approaches—cannot capture. Here, we introduce a meta-graph that helps us to discover an exact mapping between linear physical networks and independent sets, which is a central concept in graph theory. The mapping allows us to analytically derive both the onset of physical effects and the emergence of a jamming transition, and to show that physicality affects the network structure even when the total volume of the links is negligible. Finally, we construct the meta-graphs of several real physical networks, which allows us to predict functional features, such as synapse formation in the brain connectome, that agree with empirical data. Overall, our results show that, to understand the evolution and behaviour of real complex networks, the role of physicality must be fully quantified.

"物理性对网络结构的影响"
提出了"元图"meta-graph理论框架
首次建立了
物理网络与图论中"独立集"的精确映射，
为解析物理网络的演化规律
、拥堵相变
、功能预测
提供了量化工具

传统网络科学："邻接矩阵"为工具：节
点间的连接关系
现实中："有体积、不可交叉"的物
理实体，
这种"物理性"会直接影响网络的形
成与演化。

Physical networks, describing molecular and composite networks in metamaterials[1], the hard-wiring of transistors in a computer chip, the brain connectome[2] or the vascular system[3,4], are networks whose nodes and links are physical entities with defined shape and volume that cannot cross each other[5,6]. Although network science offers a suite of tools to quantify abstract networks, whose structure is fully defined by their adjacency matrix[7–11], these tools are insufficient if we wish to account for the impact of physicality. Indeed, physical networks differ from abstract networks in two key aspects. First, the nodes and links are embedded in a three-dimensional (3D) Euclidean space, and hence, similarly to spatial networks[12,13], we must specify node positions and link routing. The second and the most defining feature of physicality is volume exclusion, that is, the fact that the nodes and links are not allowed to overlap[14,15]. Although recent experimental advances have provided increasingly accurate maps of physical networks, we lack a formalism to expand the toolset of network science to these systems and to understand how physicality affects the structure and the evolution of physical networks.

物理网络的两大核心特征，也是传统模型的短板：
空间嵌入性；
体积排他性：

Here we unveil the impact of physicality through the discovery of an exact mapping of a physical network into the independent sets of a deterministic meta-graph[16], which allows us to analytically predict the onset of physicality and the emergence of a jamming transition. The formalism allows us to construct the meta-graph for real physical networks and to predict their functional features, such as synapse formation in the brain.

Linear physical network model

基础模型：线性物理网络 (LPNs)

To understand the impact of physicality on network structure, we aim to construct the simplest possible model that captures the role of volume exclusion. For this reason, we eliminated all complexities that would affect our ability to explore the role of volume exclusion, such as the curving of the links or the impact of the node volume, which prompted us to focus on linear physical networks (LPNs), whose nodes are zero-volume points in the 3D space and links are straight cylinders with diameter λ.

To generate a random λ-physical network $\mathcal{G}(\lambda, \mathcal{P})$, we started from a random finite point set $\mathcal{P}$ placed in $\mathbb{R}^3$. The points in $\mathcal{P}$, which served as nodes, were placed uniformly randomly within the unit cube with the

[1]Department of Network and Data Science, Central European University, Vienna, Austria. [2]Alfréd Rényi Institute of Mathematics, Budapest, Hungary. [3]Institute of Physics, Belgrade, Serbia. [4]Network Science Institute, Northeastern University, Boston, MA, USA. [5]Department of Medicine, Brigham and Women's Hospital, Harvard Medical School, Boston, MA, USA. [6]These authors contributed equally: Márton Pósfai, Balázs Szegedy. ✉e-mail: barabasi@gmail.com

学界缺乏统一的理论框架来量化"物理性"对网络结构的影响 —— 这正是论文要解决的核心问题

constraint that any two nodes had to be at least at λ distance from each other. To construct the network, we first chose two unconnected nodes in $\mathcal{P}$ at random and connected them by a capped cylinder of thickness λ. If the cylinder did not cross any preexisting link (except those connected to the two end nodes), we added it to the network; if, however, the proposed link overlapped with a previously added link, we deleted the proposed link and selected another random node pair to connect.

For $\lambda = 0$, we lacked physical constraints and any point pair could be connected by a link. Consequently $\mathcal{G}(0, \mathcal{P})$ mapped exactly into the Erdős–Rényi model and led to a fully connected network at $M = N(N-1)/2$, where M is the number of links and N is the number of nodes in the network. For any $\lambda > 0$, however, physicality induces a jammed state, which implies that once we reached a maximal number of links $M_{\max}(\lambda)$, no further links could be added without violating volume exclusion. To characterize the jamming process, we measured $\langle l \rangle$, the average length of the successfully added links, for different λ values (Fig. 1e). For $\lambda = 0$, all links are accepted, and hence the average length of the observed links is $l_{rs} \approx 0.662$, which is the length of a randomly selected segment from the unit cube (dashed line in Fig. 1e). For $\lambda > 0$, the measured link length $\langle l \rangle$ deviated from l_{rs} for large M, which indicates that long links often violate physicality, and the larger the value of λ, the earlier physicality manifests itself.

As Fig. 1e indicates, both the onset of physicality (M_{phys}, which captures the moment at which volume exclusion starts to play a role) and the jammed state ($M_{\max}$) decrease with increasing link diameter λ. Although $M_{\max}$ and M_{phys} are driven by random processes, we find that their values obtained for multiple independent networks generated with the same ($\lambda, \mathcal{P}$) parameters are narrowly distributed (Fig. 1f,g), which indicates that M_{phys} and $M_{\max}$ are self-averaging (Supplementary Information Section 3.2). Our goal, therefore, is to unveil the processes that govern these variables, which will help us to understand the impact of physicality on the network structure.

Meta-graph and independent sets

To uncover the dependence of the onset of physicality (M_{phys}) and the jamming transition ($M_{\max}$) on the link thickness λ and the number of nodes $N = |\mathcal{P}|$, we introduced the meta-graph $\mathcal{M}(\mathcal{P}, \lambda)$, which is designed to capture the physical constraints among the link candidates. The meta-graph has $N(N-1)/2$ vertices, each corresponding to a possible link (p_i, p_j) between the N nodes. Two links (p_1, p_2) and (p_3, p_4), corresponding to two vertices of the meta-graph, are connected if they violate physicality, that is, if the distance between the line segments (p_1, p_2) and (p_3, p_4) is below λ (Fig. 1a–d). Note that, for a given point set $\mathcal{P}$ and link thickness λ, the construction of the meta-graph $\mathcal{M}(\mathcal{P}, \lambda)$ is fully deterministic.

The value of the meta-graph stems from the discovery that any LPN $\mathcal{G}(\mathcal{P}, \lambda)$ corresponds to an independent set of vertices in $\mathcal{M}(\mathcal{P}, \lambda)$ and vice versa. A set of vertices is called independent if there are no edges between the elements of the set (Fig. 2a,b). For example, each vertex of the meta-graph of Fig. 1b,d corresponds to a potential link of the physical networks of Fig. 1a,c. The meta-vertices shown in red in Fig. 1b,d form independent sets, as there are no direct edges between them. Therefore, each link in the physical network that corresponds to a red meta-vertex can coexist with any other link corresponding to another red meta-vertex, as they do not violate physicality.

Independent sets are extensively studied in combinatorics[16], computer science[17], probability theory and statistical physics[18,19]. The exact mapping between a λ-physical network $\mathcal{G}(\mathcal{P}, \lambda)$ and the independent vertex sets of the $\mathcal{M}(\mathcal{P}, \lambda)$ is our key result that, as we show next, allows us to develop an analytically solvable formalism to explore the structure and the evolution of physical networks.

Predicting the evolution of physical networks

We rely on the mapping between λ-physical networks and the independent sets of meta-graphs to derive M_{phys} and $M_{\max}$ and to understand the role of physicality. We must account for two limits as
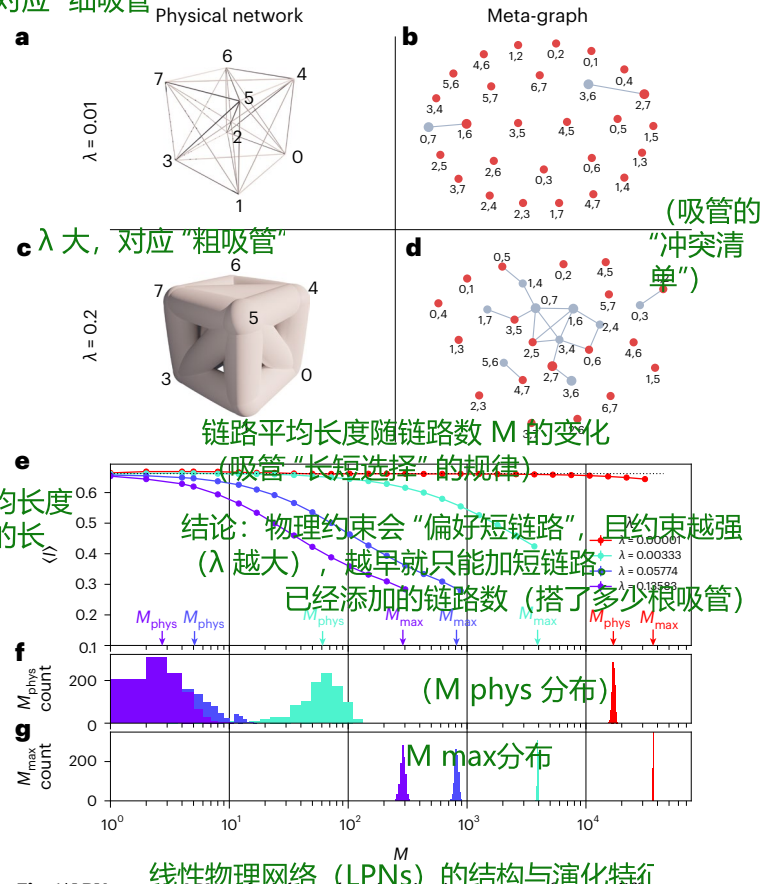

Fig. 1 | LPNs. a,c, An LPN with eight nodes, showing its structure for two different λ values. Although for the small λ (**a**) most links are allowed, for $\lambda = 0.2$ (**c**) many links are forbidden, as they would overlap with other links. **b,d,** The 28 vertices of the meta-graph represent the candidate links of the physical network for $\lambda = 0.01$ (**b**) and for $\lambda = 0.2$ (**d**), each labelled by the node numbers they attempt to connect. Two vertices are connected if the corresponding links overlap, and hence they cannot coexist in a physical network. Each independent vertex set of these meta-graphs corresponds to a valid physical network: the independent set formed by the red nodes represents the physical network shown in **a** and **c**. **e–g,** To model the evolution of a LPN, we generated a point set $\mathcal{P}$ with $N = 300$ nodes, randomly adding links if they did not violate λ-physicality, and repeated the process 1,000 times for the same $\mathcal{P}$. **e,** The observed length of the links after the addition of M links. The data points are logarithmically spaced and the dashed line corresponds to $l_{rs} \approx 0.662$, which is the expected length of a random segment chosen from the unit cube (expected for $\lambda = 0$). The higher the value of λ, the more conflicts links have, and hence the more the observed l deviated from l_{rs}. Error bars representing the standard error of the mean (SEM) are smaller than the marker size. **f,g,** Histogram of M_{phys} (**f**) and $M_{\max}$ (**g**) for different realizations, showing that M_{phys} and $M_{\max}$ are concentrated on a narrow range, being largely independent of the order in which the links are added. Owing to the logarithmic scale, the histograms for low M_{phys} and $M_{\max}$ appear to be wider. In simulations, we measured M_{phys} as the number of links above which at least one-sixth of the link candidates were rejected. (Supplementary Information Section 1.5.5).

we proceed: (1) with fixed λ, we cannot take the large network limit ($N \to \infty$) because the total volume of the links, whose lower bound scales as $N\lambda^3$ for networks with non-vanishing average degree, exceeds the available volume for large N, which results in a disconnected network. Therefore, we must decrease λ as we increase N to ensure that $\lambda \lesssim N^{-1/3}$; and (2) if λ decreases too fast with N, the average meta-degree $\langle k_{meta} \rangle \approx \lambda N^2$ (Supplementary Information Section 1.4) converges to zero and physicality will stop playing a role, which implies that $\lambda \gtrsim N^{-2}$. To satisfy (1) and (2), we set

$$\lambda = \frac{C}{N^\alpha}, \tag{1}$$

where C is an arbitrary constant and the control parameter α interpolates between the crowded state (1, $\alpha = 1/3$) and the loss of physicality (2, $\alpha = 2$).

We began by observing that the construction of a random LPN is equivalent to building a greedy independent set $\mathcal{I}$ of $\mathcal{M}(\mathcal{P}, \lambda)$ by sequentially selecting the meta-vertices in random order and adding the tth meta-vertex to $\mathcal{I}$ if none of its neighbours are in $\mathcal{I}$. To analytically characterize this process, we introduced a randomized reference meta-graph $\mathcal{M}_{rr}(\mathcal{P}, \lambda)$ in which two link candidates with length l_1 and l_2 were connected independently with probability $(\pi/2)\lambda l_1 l_2$, to represent the approximate probability that the distance between two randomly selected segments of lengths l_1 and l_2 was at most λ. This construction provided a first-order approximation of $\mathcal{M}(\mathcal{P}, \lambda)$ in λ: the expected degree of a vertex with length l was ~λl in both $\mathcal{M}(\mathcal{P}, \lambda)$ and $\mathcal{M}_{rr}(\mathcal{P}, \lambda)$ in leading order, whereas higher-order structures, such as the number of triangles in which a vertex participates, are not captured by $\mathcal{M}_{rr}(\mathcal{P}, \lambda)$. We then leveraged $\mathcal{M}_{rr}(\mathcal{P}, \lambda)$ to derive a differential equation that governed the temporal evolution of the total length $L_{total}(t)$ of links in $\mathcal{I}$ (ref. [20]) (Supplementary Information Section 3)

$$\dot{L}_{total}(\tau) = \frac{N^2}{2} \int_0^{\sqrt{3}} l \exp\left[-\frac{\pi}{2}\lambda L_{total}(\tau)l\right] p_{LC}(l)\mathrm{d}l, \qquad (2)$$

where $\tau = 2t/N(N-1)$ is the rescaled time and $p_{LC}(l)$ is the length distribution of the link candidates. The expression $\exp\left[-\frac{\pi}{2}\lambda L_{total}(\tau)l\right]$ is the probability that a meta-vertex with length l has no connections leading to the independent set $\mathcal{I}$ at τ. This means that the acceptance of link candidates decays exponentially with l, which suggests that $p(l)$, the distribution of the length of the accepted links, also decays exponentially; this agrees with results on brain architecture that have found an exponential law[21,22]. The total link length $L_{total}(\tau)$, however, increases over time, which means that longer links are added earlier during the evolution of the network rather than in later stages. In fact, we predict that this source of heterogeneity leads to a power law link length distribution $p(l) \approx l^{-3}$ with an upper cut-off dictated by the finite size of the system (Supplementary Information Section 4).

The onset of physicality happens when link candidates get rejected with positive probability, that is, $\lambda L_{total}(\tau) \to$ constant for $N \to \infty$, which predicts that

$$M_{phys} \approx N^{\alpha}, \qquad (3)$$

unveiling that the control parameter α directly governs the onset of physicality M_{phys}. Equation (2) also predicts that the jamming point scales as

$$M_{max} \approx N^{\frac{3\alpha+4}{5}}, \qquad (4)$$

and the total link length in the jammed state scales as

$$L_{total} \approx N^{\frac{4\alpha+2}{5}}. \qquad (5)$$

Equation (2) allows us to study the fluctuations of these quantities, which yields that their variances scale as $\sigma^2(M_{phys}) \approx N^{\alpha}$, $\sigma^2(M_{max}) \approx N^{\frac{3\alpha+4}{5}}$ and $\sigma^2(L_{total}) \approx N^{\alpha} \ln N$. Consequently, in the large network limit, the typical fluctuations converge to zero compared with their expectation, which indicates that equations (3)–(5) correctly capture the typical behaviour of LPNs.

Our analytical predictions are directly testable by simulations. We began by numerically solving equation (2) to determine the dependence of M_{max} on λ (Fig. 2c), and we found excellent agreement, particularly for small λ. Next, we tested the predicted scaling behaviour given in equations (3)–(5) by constructing LPNs of increasing sizes, and we found that they offer an accurate description of the onset of physicality (Fig. 2c–e). The predictive accuracy of equation (2) indicates that the likelihood of adding a physical link to the network is driven primarily by the length of the link, and hence higher-order effects, such as the formation of triangles, which are ignored by $\mathcal{M}_{rr}(\mathcal{P}, \lambda)$, play a negligible role.

Figure 2g summarizes the behaviour of physical networks as predicted by equations (2)–(5), and it documents the vanishing role of physicality with increasing α.

For $\alpha < 1/3$, the link widths are larger than the typical distance between adjacent nodes, and hence the network remains disconnected. The first realizable network emerges for $\alpha = 1/3$, in which case equation (3) predicts that $M_{phys} \approx N^{1/3}$, which means that physicality plays a role even when the network is ultra sparse ($\langle k \rangle = 2M_{phys}/N \approx N^{-2/3} \to 0$). For $\alpha = 1/3$, we have $M_{max} \approx N$, which indicates that the jammed network is also sparse ($\langle k \rangle = O(1)$). The link length in the jammed network $l^* \approx L_{total}/M_{max}$ is of the order of the distance between physically adjacent nodes ~$N^{-1/3}$.

Between $1/3 \le \alpha \le 2$, we are in the physical regime, with two subregimes: in the sublinear regime ($1/3 < \alpha \le 1$), physicality plays a role even in sparse networks ($\langle k \rangle = O(1)$). In contrast, in the superlinear regime ($1 < \alpha \le 2$), sparse LPNs are not affected by physicality, and hence we need a superlinear number of links before physicality affects network formation.

Finally, for $\alpha = 2$, the onset of physicality scales as $M_{phys} \approx N^2$ and $M_{max} \approx N^2$, which means that physical interactions are only important in dense networks. The average physical link length $\langle l \rangle$ in this regime is of the order of the system size, indicating that the links can span the entire system, which is a consequence of the vanishing role of physical effects.

The adjacency matrix in the jammed state is predictive of node positions

A key prediction of our formalism is that physicality affects the structure of networks even with vanishing volume. Indeed, according to equation (5), the network volume scales as $V \approx \lambda^2 L_{total} \approx N^{-\frac{6\alpha-2}{5}}$, and hence, in the $N \to \infty$ limit for any $\alpha > 1/3$, the jammed network occupies a zero fraction of the available space.

As the number of links increases, so does the number of physical constraints that each new link must satisfy. Hence, our ability to place a new link becomes increasingly dependent on the existing links, which, in turn, leads to correlations between the adjacency matrix and the physical layout of the network. Indeed, before physicality turns on ($M < M_{phys}$), the distribution of eigenvalues follows Wigner's semicircle law (Fig. 3a)[23]. When, however, the number of links M approaches the jammed state M_{max}, three additional eigenvalues μ_2, μ_3 and μ_4 separate from the bulk (Fig. 3b). In non-physical networks, such eigenvalues often indicate the presence of a large-scale organization in the network: for example, leading eigenvectors may correspond to a macroscopic community structure[24]. In contrast, in physical networks the leading eigenvectors are induced by physicality, which signals a strong spatial dependence: the typical link length $l^* \approx L_{total}/M_{max} \approx N^{-\frac{2-\alpha}{5}}$ decreases with increasing N and nodes are densely connected in their l^* neighbourhood, whereas the majority of long-range links are suppressed. The resulting large-scale 3D spatial organization is captured by the eigenvalues μ_2, μ_3 and μ_4 and the corresponding eigenvectors $\mathbf{v}^{(2)}$, $\mathbf{v}^{(3)}$ and $\mathbf{v}^{(4)}$: the eigenvectors at node i become strongly correlated with the spatial coordinates of i. In other words, as we approach the jammed state, the adjacency matrix becomes predictive of the position of individual nodes. To quantify the predictive power of the leading eigenvectors, we rotated $\mathbf{v}^{(2)}$, $\mathbf{v}^{(3)}$ and $\mathbf{v}^{(4)}$ to best align with the node coordinates and we calculated the coefficient of determination: that is, we measured how well $(v_i^{(2)}, v_i^{(3)}, v_i^{(4)})$, the eigenvectors at node i, predicted its coordinates (x_i, y_i, z_i) (Supplementary Information Section 5.3). We found that the coefficient of determination increased rapidly as we approached the jammed state, which indicated that the node positions predicted by the adjacency matrix converged towards their true values (Fig. 3c,d). In other words, although a complete description of physical
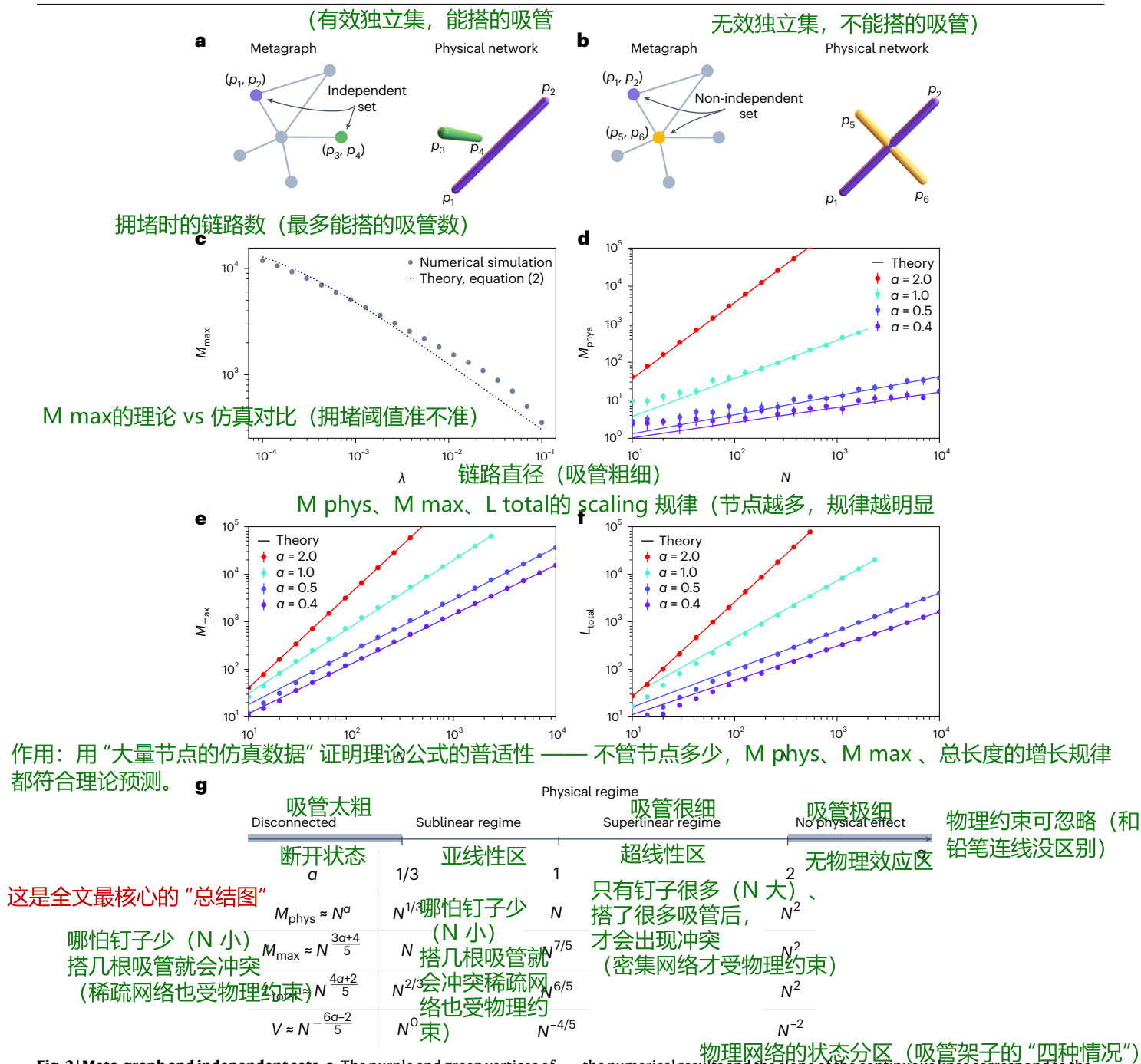
Fig. 2 | Meta-graph and independent sets. a, The purple and green vertices of the meta-graph have no direct edges between; hence they form an independent set, which indicates that the corresponding physical links (p_1, p_2) and (p_3, p_4) are non-overlapping (conflict free). **b**, The purple and yellow vertices do not form an independent set, because they are connected by a direct edge, which indicates that the physical links corresponding to them overlap, and hence they cannot be added simultaneously. **c**–**g**, To test the analytical predictions provided by the meta-graph, we simulated LPNs and numerically measured the number of links at the onset of physicality (M_{phys}), the maximal number of links (M_{max}) and their length (L_{tot}) in the jammed state. **c**, We compare the prediction of equation (2) with the numerical estimate of M_{max} from simulations of LPNs with $N = 200$. Markers represent the average of 50 independent networks, and the error bars representing the SEM are smaller than the marker size. **d**–**f**, We show Mphys (d), Mmax (e) and Ltot (f) for LPNs with increasing N and link thickness scaling as $\lambda = C/N^\alpha$. The symbols indicate

the numerical results and the slope of the continuous lines correspond to the scaling exponents predicted by equations (3)–(5). The data points represent an average of ten independent runs and the error bars representing the SEM are typically smaller than the marker size. **g**, The behaviour of physical networks as a function of α. For $\alpha < 1/3$, the links are wider than the typical distance between physically adjacent nodes, which leads to disconnected physical networks with zero average degree in the $N \to \infty$ limit. In contrast, for $\alpha > 2$, the role of physicality vanishes. Between these two limits, physicality affects the formation of networks with more than $M_{phys} \approx N^\alpha$ links. For $1/3 \le \alpha \le 1$, physicality turns on after the addition of a sublinear number of links and therefore even sparse networks ($M \approx N$) are affected by physicality. In contrast, for $1 \le \alpha \le 2$, volume exclusion has an effect only after the addition of a superlinear number of links, and hence only dense networks are affected by physicality. Overall, the role of physicality weakens for increasing α.
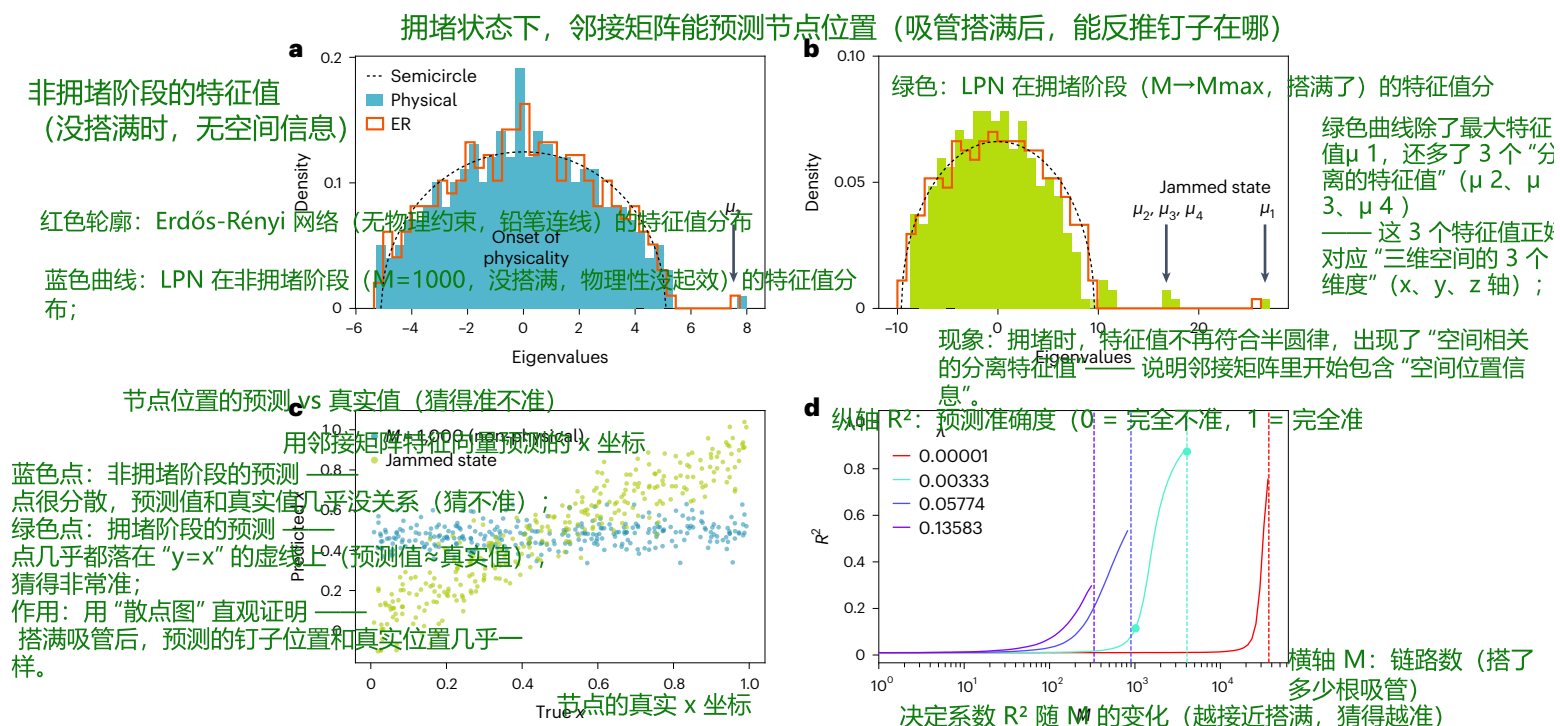
拥堵状态下，邻接矩阵能预测节点位置（吸管搭满后，能反推钉子在哪）

非拥堵阶段的特征值
（没搭满时，无空间信息）

红色轮廓：Erdős-Rényi 网络（无物理约束，铅笔连线）的特征值分布

蓝色曲线：LPN 在非拥堵阶段（M=1000，没搭满，物理性没起效）的特征值分布；

绿色：LPN 在拥堵阶段（M→Mmax，搭满了）的特征值分

绿色曲线除了最大特征值 μ1，还多了 3 个"分离的特征值"（μ2、μ3、μ4）—— 这 3 个特征值正好对应"三维空间的 3 个维度"（x、y、z 轴）；

现象：拥堵时，特征值不再符合半圆律，出现了"空间相关的分离特征值"—— 说明邻接矩阵里开始包含"空间位置信息"。

节点位置的预测 vs 真实值（猜得准不准）

用邻接矩阵特征向量预测的 x 坐标

蓝色点：非拥堵阶段的预测—点很分散，预测值和真实值几乎没关系（猜不准）；
绿色点：拥堵阶段的预测—点几乎都落在"y=x"的虚线上（预测值≈真实值），猜得非常准；
作用：用"散点图"直观证明—搭满吸管后，预测的钉子位置和真实位置几乎一样。

纵轴 R²：预测准确度（0 = 完全不准，1 = 完全准）

横轴 M：链路数（搭了多少根吸管）

决定系数 R² 随 M 的变化（越接近搭满，猜得越准）

Fig. 3 | Predicting node positions in the jammed state. a, The spectral density of the adjacency matrix for $N = 300$ and $\lambda = 1/N$ after the addition of $M = 1000$ links (blue). Before the onset of physicality, the eigenvalues of the LPN are consistent with an Erdős-Rényi (ER) network of the same size (red outline): the bulk of the spectral density is well approximated by Wigner's semicircle law (dashed line) and the largest eigenvalue separated from the bulk (μ_1) corresponds to the average degree of the network. **b**, In the jammed state, the eigenspectrum of the LPN (green) deviates from the spectrum of an ER network (red outline): three additional eigenvalues μ_2, μ_3 and μ_4 become separated from the bulk as a consequence of physical interactions. **c**, Comparing the predicted and the true x coordinate of each node shows that, although for small link density the adjacency matrix has no predictive power (blue symbols), the adjacency matrix can reliably predict the position of nodes in the jammed state (green symbols). **d**, The coefficient of determination R^2 increased as we added links to the LPNs, which indicates that, as we approached the jammed state, the predictive power of the adjacency matrix increased. The circles highlight the R^2 values corresponding to the λ shown in **a** and **b**. Subplots **a**–**c** show results for a single LPN and **d** shows the average of 1,000 independent networks.

networks requires simultaneous information on the adjacency matrix, link routing and node layout, we found, unexpectedly, that in the jammed state, where physicality is the strongest, these features become so intertwined that the adjacency matrix alone offers a complete description of the system. Note that having reduced space around nodes does not on its own imply predictability: for example, the adjacency matrix of a densely packed tree does not carry any information about the physical location of the nodes, as such networks can be folded into a volume in many different ways, which changes the layout but preserves the abstract network.

The meta-graph of real networks

While the LPN model conceptualizes physical networks as nodes connected by straight links, in real physical networks, such as the brain connectome or the vascular network, the links curve. As we show next, the meta-graph offers a quantitative framework to characterize the impact of physicality for networks with arbitrary link shapes and structure.

In their native state, neurons in the brain or the vessels of a vascular network obey volume exclusion. If, however, we increase the thickness λ of all links by a $\Delta\lambda$, conflicts can emerge. Therefore, we defined a generalized meta-graph $\mathcal{M}_g(\Delta\lambda)$, in which we connected two vertices of the meta-graph if the corresponding physical objects (links or nodes) overlapped for a given $\Delta\lambda$, concisely capturing the spatial organization of a physical network (Supplementary Information Section 7).

We constructed $\mathcal{M}_g(\Delta\lambda)$ for multiple real physical networks, including the fruit fly's brain[2], the vascular network of a mouse[4] and a mitochondrial network[25]. We illustrate the process in Fig. 4a, which shows the meta-graph of the fruit fly connectome, which consists of $N = 2,970$ neurons and $M = 35,707$ synapses serving as links.

According to Peter's rule, neurons can only form synapses if their axons and dendrites are in close physical proximity[26,27]. Hence, we expected and found a strong correlation between the meta-degree and the number of synapses (Supplementary Fig. 21). To abstract from these obvious correlations between the generalized meta-graph and synapse formation, we focused only on conflicts between neurons that are not connected by synapses and therefore are the result of the packing of the neurons in the brain. We achieved this by building a restricted meta-graph, where we removed the synaptically connected links from the meta-graph. Figure 4a highlights the vertex with the highest restricted meta-graph degree $k_A = 13$, corresponding to the most physically confined neuron, bordered by 13 other neurons that it does not synapse with (Fig. 4b,c). This prompts the following question. Is the most confined neuron also the most central in the synaptic network? To find an answer, we performed a linear regression between the restricted meta-degree and the logarithm of synapses, which revealed a positive association between the physical confinement and the functional role of neurons (Fig. 4d, slope $a = 0.356 \pm 0.022$ and $R^2 = 0.26$). Our result indicates that synaptically central neurons in the connectome are tightly confined in the brain by non-synaptic partners. This is not obvious, as we can construct physical networks that have negative correlations between the number of synapses and the restricted meta-degree: consider a physical network with N nodes where each neuron is physically adjacent to all $N-1$ other neurons (Supplementary Fig. 23). If a neuron i has k synaptic partners, then it has $N-1-k$ meta-degree, which results in a perfect anticorrelation between the number of synapses and the meta-degree. Overall, the observed correlations confirm that the meta-graph captures important properties of the physical layout and
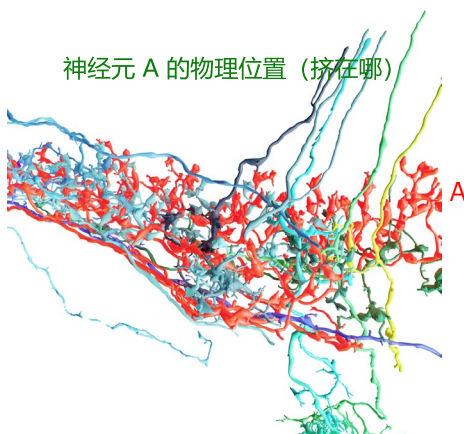
a

红色顶点（神经元 A）：受限元图中"度最高"的
神经元 —— 和 13 个非突触神经元物理重叠（被
13 个神经元挤着）；
灰色顶点：1469 个"孤立顶点"—— 没有和任何非
突触神经元重叠（不挤）；
作用：构建真实网络的"物理冲突清单"，找出
"物理上最挤的神经元"。
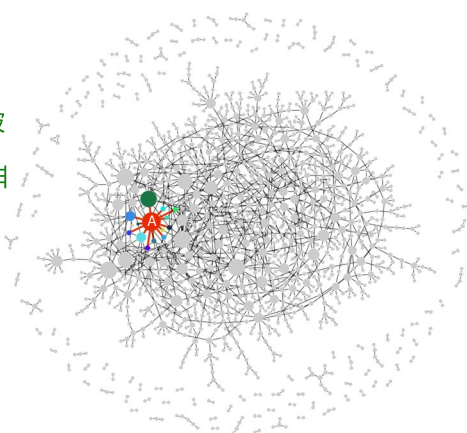
果蝇大脑的"受限元图"（只看物理冲
突的非突触神经元）

b

神经元 A 的物理位置（挤在哪）

A

c

拥挤不是整体的，是局部区域
的物理冲突
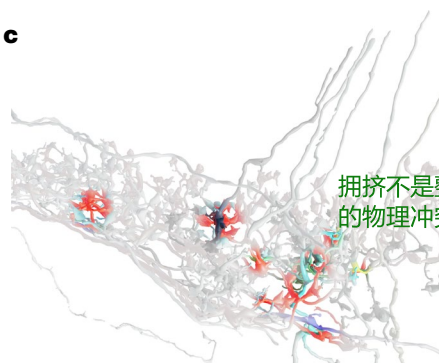
物理拥挤度越高的神经元，突触数量越多 —— 说明"大脑
中功能重要的神经元，反而物理上更拥挤"

d

神经元的突触数量（功能重要性）

e

小点点是单个神经元，大点点是"按拥挤
度分组的平均值"

结论：元图能揭示"物理约束"和"功能连接"的关联
—— 这是传统网络模型做不到的，证明理论框架对真实
科学问题有价值。
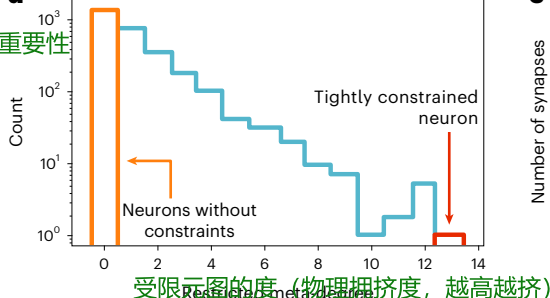
受限元图的度（物理拥挤度，越高越挤）
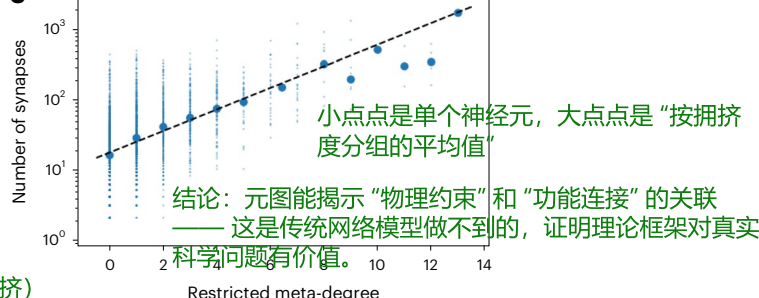
Fig. 4 | Meta-graph of real networks. a, Each vertex of the restricted meta-graph represents a neuron in the fruit fly connectome[2]. A link between two vertices of the restricted meta-graph implies that the corresponding neurons overlap if we increase their thickness by $\Delta\lambda \approx 0.028$ but they are not connected by synapses. The neuron with the highest restricted meta-degree, A, has 13 connections, whereas 1,469 isolated vertices (not shown) correspond to neurons that are conflict free for $\Delta\lambda \approx 0.028$. **b**, Neuron A (red) has the most excess confinement. We show it together with the 13 neurons that are within distance $\Delta\lambda$ of A, and hence are connected to A in the restricted meta-graph and are highlighted in **a**. The neuron colours match the colours of the meta-vertices in **a**. **c**, Neuron A is an extended, physical object, whose physical conflicts with other neurons are localized in specific neighbourhoods of the physical network, as highlighted in the figure. **d**, The degree distribution of the restricted meta-graph for $\Delta\lambda \approx 0.028$.

Vertices with degree zero correspond to conflict-free neurons, that is, lack proximity within $\Delta\lambda$ with other neurons that are not connected to them by means of synapses. Physically confined neurons have high restricted meta-degree, which is indicative of a large number of physical conflicts. **e**, The dependence of the restricted meta-degree on the number of synapses of each neuron indicates that the restricted meta-degree is predictive of synapse formation. The dashed line corresponds to linear regression between the restricted meta-degree and the logarithm of the number of synapses for each neuron. Small markers represent individual neurons; large markers are binned averages. For illustration purposes, we chose $\Delta\lambda$ such that the meta-graph is sparse. In Supplementary Information Section 7, we repeat the above analysis for various $\Delta\lambda$ values and find that the positive association between the restricted meta-graph and the synaptic network is robust.

can be used to systematically study the connection between physical and abstract network structure.

As connectome mapping aspires to scale up to the 10^9 neurons of the human brain, new mathematical and computational formalisms, such as the one offered by the meta-graph, are needed to unveil the predictive power of these exceptionally large physical network maps. Full description of the layout of a physical network requires

copious amounts of data that is difficult to handle computationally and also limits analytical advances. For example, the Hemibrain dataset describes the 3D trajectory of approximately 25,000 neurons of a fruit fly using 117 million linear segments[2]. Naïve identification of physical conflicts, therefore, requires 10^{16} distance computations, which is a prohibitive computational burden for most researchers. In contrast, the $25,000 \times 25,000$ adjacency matrix of the generalized meta-graph

can be represented using a few hundred megabytes of data, and hence publishing it together with the adjacency of the connectome would allow the computationally efficient study of the relationship between physical and abstract network structure.

Discussion

Recent experimental advances, driven by connectomics and high-resolution magnetic resonance imaging, have offered detailed and accurate maps of a wide range of physical networks, from the structure of individual neurons in a brain to 3D maps of large vascular systems. These advances unveiled an important gap in network science: the lack of understanding of how physicality affects the network structure. The need for a quantitative and conceptual framework goes beyond biology: complex metamaterials, combining random and repetitive local structures[1,28,29], offer other manifestations of physical networks and so do computer chips that pack billions of transistors. Here we introduce a formalism designed to systematically explore the structure of physical networks. We show that the impact of physicality is not limited to dense networks—on the contrary, in their jammed state, physical networks are sparse, with the relative volume of their links converging to zero for large systems. In other words, physicality is not a simple manifestation of crowding, but has subtle and non-trivial consequences on the network structure. The advances presented here raise multiple open questions, many of which can be addressed using meta-graphs. For example, many real networks are characterized by non-uniform node density, heterogeneous link diameters and bent links, and are potentially affected by the order in which the nodes and the links are added to the network. The impact of these features can be studied by extending the random LPN model or using the generalized meta-graphs. These variants of LPNs may serve as null models for understanding the features of the physical layout and network structure of real systems (Supplementary Information Section 7.6). Other issues are less straightforward extensions of our work, but may benefit from the meta-graph framework: for example, understanding the effect of the physical architectures on network robustness[30,31] or on dynamics on networks[32–36].

A quantitative understanding of physicality can have a direct impact on multiple areas of science. For example, at this point, it is unclear to what degree the observed brain connectomes are driven by the genetic processes that govern their developmental biology[37] or by physical constraints that the neurons and their interactions must obey, which limit a neuron's ability to synapse with desired target neurons in a very dense environment. Answers require a modelling and analytical platform that helps us to systematically explore the competing role of genetics and physicality.

Online content

Any methods, additional references, Nature Portfolio reporting summaries, source data, extended data, supplementary information, acknowledgements, peer review information; details of author contributions and competing interests; and statements of data and code availability are available at https://doi.org/10.1038/s41567-023-02267-1.

References

1. Kadic, M., Milton, G. W., van Hecke, M. & Wegener, M. 3D metamaterials. *Nat. Rev. Phys.* **1**, 198–210 (2019).
2. Scheffer, L. K. et al. A connectome and analysis of the adult drosophila central brain. *eLife* **9**, e57443 (2020).
3. Banavar, J. R., Maritan, A. & Rinaldo, A. Size and form in efficient transportation networks. *Nature* **399**, 130 (1999).
4. Gagnon, L. et al. Quantifying the microvascular origin of bold-fMRI from first principles with two-photon microscopy and an oxygen-sensitive nanoprobe. *J. Neurosci.* **35**, 3663 (2015).
5. Dehmamy, N., Milanlouei, S. & Barabási, A.-L. A structural transition in physical networks. *Nature* **563**, 676 (2018).
6. Liu, Y., Dehmamy, N. & Barabási, A.-L. Isotopy and energy of physical networks. *Nat. Phys.* **17**, 216 (2021).
7. Dorogovtsev S. N. & Mendes J. F. *Evolution of Networks: From Biological Nets to the Internet and WWW* (Oxford Univ. Press, 2003).
8. Caldarelli G. *Scale-free Networks: Complex Webs in Nature and Technology* (Oxford Univ. Press, 2007).
9. Cohen R. & Havlin S. *Complex Networks: Structure, Robustness and Function* (Cambridge Univ, Press, 2010).
10. Newman M. *Networks: An Introduction* (Oxford Univ. Press, 2010).
11. Barabási A.-L. *Network Science* (Cambridge Univ. Press, 2016).
12. Barthélemy, M. Spatial networks. *Phys. Rep.* **499**, 1 (2011).
13. Horvát, S. et al. Spatial embedding and wiring cost constrain the functional layout of the cortical network of rodents and primates. *PLoS Biol.* **14**, e1002512 (2016).
14. Rubinstein M. et al. *Polymer Physics*, Vol. 23 (Oxford Univ. Press New York, 2003).
15. Song, C., Wang, P. & Makse, H. A. A phase diagram for jammed matter. *Nature* **453**, 629 (2008).
16. West D. B. et al. *Introduction to Graph Theory*, Vol. 2 (Prentice Hall, 2001).
17. Tarjan, R. E. & Trojanowski, A. E. Finding a maximum independent set. *SIAM J. Comput.* **6**, 537 (1977).
18. Flory, P. J. Intramolecular reaction between neighboring substituents of vinyl polymers. *J. Am. Chem. Soc.* **61**, 1518 (1939).
19. Hartmann A. K. & Weigt M. *Phase Transitions in Combinatorial Optimization Problems: Basics, Algorithms and Statistical Mechanics* (Wiley, 2006).
20. Brightwell, G., Janson, S. & Luczak, M. The greedy independent set in a random graph with given degrees. *Random Struct. Algorithms* **51**, 565 (2017).
21. Ercsey-Ravasz, M. et al. A predictive network model of cerebral cortical connectivity based on a distance rule. *Neuron* **80**, 184 (2013).
22. Bassett, D. S. & Bullmore, E. T. Small-world brain networks revisited. *Neuroscientist* **23**, 499 (2017).
23. Van Mieghem P. *Graph Spectra for Complex Networks* (Cambridge Univ. Press, 2010).
24. Abbe, E. Community detection and stochastic block models: recent developments. *J. Mach. Learn. Res.* **18**, 6446 (2017).
25. Viana, M. P. et al. Mitochondrial fission and fusion dynamics generate efficient, robust, and evenly distributed network topologies in budding yeast cells. *Cell Syst.* **10**, 287 (2020).
26. Rees, C. L., Moradi, K. & Ascoli, G. A. Weighing the evidence in Peters' rule: does neuronal morphology predict connectivity? *Trends Neurosci.* **40**, 63 (2017).
27. Udvary, D. et al. The impact of neuron morphology on cortical network architecture. *Cell Rep.* **39**, 110677 (2022).
28. Nicolaou, Z. G. & Motter, A. E. Mechanical metamaterials with negative compressibility transitions. *Nat. Mater.* **11**, 608 (2012).
29. Kim, J. Z., Lu, Z., Blevins, A. S. & Bassett, D. S. Nonlinear dynamics and chaos in conformational changes of mechanical metamaterials. *Phys. Rev. X* **12**, 011042 (2022).
30. D'Souza, R. M., Gómez-Gardenes, J., Nagler, J. & Arenas, A. Explosive phenomena in complex networks. *Adv. Phys.* **68**, 123 (2019).
31. Heroy, S., Taylor, D., Shi, F., Forest, M. G. & Mucha, P. J. Rigidity percolation in disordered 3D rod systems. *Multiscale Model. Sim.* **20**, 250 (2022).
32. Barrat, A., Barthelemy, M. & Vespignani A. *Dynamical Processes on Complex Networks* (Cambridge Univ. Press, 2008).
33. Ulloa Severino, F. P. et al. The role of dimensionality in neuronal network dynamics. *Sci. Rep.* **6**, 1 (2016).

图 1：先展示 "物理网络的基本现象"（λ 影响结构、Mphys和Mmax稳定）；
图 2：用 "元图 - 独立集" 解释现象，并验证理论公式的正确性（预测准不准、规律普不普适）；
图 3：挖掘理论的 "意外价值"（拥堵时能反推节点位置）；
图 4：把理论用到真实网络（果蝇大脑），解决实际科学问题（物理 vs 功能的关联）。

34. Bianconi G. *Multilayer Networks: Structure and Function* (Oxford Univ. Press, 2018).

35. Case, D. J., Liu, Y., Kiss, I. Z., Angilella, J.-R. & Motter, A. E. Braess's paradox and programmable behaviour in microfluidic networks. *Nature* **574**, 647 (2019).

36. Kim, J. Z., Lu, Z., Strogatz, S. H. & Bassett, D. S. Conformational control of mechanical networks. *Nat. Phys.* **15**, 714 (2019).

37. Kovács, I. A., Barabási, D. L. & Barabási, A.-L. Uncovering the genetic blueprint of the *C. elegans* nervous system. *Proc. Natl Acad. Sci. USA* **117**, 33570 (2020).

1

传统方法："为什么有些神经元能连，有些不能连"（明明距离近，却没突触）？
更无法预测 "这样的网络最多能连多少条线"（比如大脑里神经元会不会 "挤到连不下新突触"）。

传统工具 "忽略了物理约束"，面对真实物理网络时 "失灵" 了 —— 这就是论文要解决的 "核心痛点"。

2　　解决思路：先简化，再创新工具

1. 第一步：简化模型 —— 线性物理网络（LPNs）
为了聚焦 "不能交叉" 这个核心物理约束，论文把复杂的物理网络简化成 "最干净的版本"（对应图 1a、c）：
节点：无体积的点（不用考虑神经元本身的大小）；
链路：直的、有固定粗细 λ 的圆柱（不用考虑血管弯曲、神经元轴突拐弯）；
规则：连新链路时，只要不与已有的链路交叉，就保留；交叉就扔掉。
这个简化模型的好处是：排除了所有干扰（比如链路弯曲、节点体积），只留下 "体积排他" 这一个核心变量 —— 就像
研究 "吸管怎么搭不交叉" 时，先只用 "直吸管、小钉子"，不考虑吸管弯了、钉子太大的情况。

2. 第二步：发明工具 —— 元图（meta-graph）与独立集
简化后，问题变成 "怎么用数学描述'吸管不交叉'"—— 论文的核心创新就在这：把 "物理约束" 转化成 "数学问题"（对
应图 2a、b）。
先做一张 "所有可能的吸管清单"：比如有 4 个钉子，清单里就有 AB、AC、AD、BC、BD、CD 6 根候选吸管（这就
是元图的 "顶点"）；
再画 "冲突线"：如果两根吸管交叉（比如 AB 和 CD 交叉），就在清单上这两根吸管之间画一条线（这就是元图的
"边"）；
最后发现："能一起搭的吸管组合"（不交叉），正好是元图里的 "独立集"（独立集 = 一组顶点，彼此之间没有边，也就
没有冲突）。

这个 "元图 - 独立集" 的映射，是整个论文的 "金钥匙"—— 它把 "搭吸管会不会交叉" 这个凭感觉的物理问题，变成了
"找独立集" 这个有成熟数学方法的问题。

3　　核心发现：用工具算出物理网络的 "规律"

有了 LPNs 模型和元图工具，论文通过计算和仿真（对应图 1e-g、图 2c-f），得出了 3 条关键规律 —— 这些规
律就是 "物理网络的说明书"：
　　　　　　　　1. 规律 1：链路越粗（λ 越大），越早 "搭不动"
　　　　　　　　就像用粗吸管搭架子，很快就会交叉被拒绝（图 1e）：
　　　　　　　　物理性起效阈值Mphys：λ 越大，Mphys越小（越早开始有吸管被拒绝）；
　　　　　　　　拥堵阈值Mmax：λ 越大，Mmax越小（越早搭满，再也加不了新吸管）。

　　　　　　　　2. 规律 2：节点越多，这些阈值的增长有固定 "公式"
　　　　　　　　当节点数 N 增加时（桌子上的钉子变多），Mphys、M max、总链路长度Ltotal的增长不是乱的，
　　　　　　　　是符合固定公式（对应图 2d-f）：Mphys≈N α（α 是控制链路粗细随节点数变化的参数）；
　　　　　　　　M max≈N (3α+4)/5；L total≈N(4α+2)/5。
　　　　　　　　这些公式的价值在于：只要知道节点数 N 和链路粗细 λ，就能提前算出 "什么时候开始冲突""最多
　　　　　　　　能搭多少条线"—— 比如提前预测 "大脑里 N 个神经元最多能连多少突触"。

　　　　　　　　3. 规律 3：搭满的时候（拥堵状态），能通过 "连线" 反推 "位置"
　　　　　　　　这是最意外的发现（对应图 3）：当吸管搭满、再也加不了新的时（拥堵状态），只看 "哪两个钉子
　　　　　　　　连了吸管"（邻接矩阵），就能反推出 "钉子在桌子上的位置"。
　　　　　　　　原理：拥堵时，链路的 "连接关系" 和 "空间位置" 高度绑定 —— 比如 "连了近的钉子" 的吸管多，
　　　　　　　　"连了远的钉子" 的吸管少，这种连接规律里藏着位置信息；
　　　　　　　　应用：对大脑研究来说，"测神经元之间的突触连接" 比 "测神经元在大脑里的位置" 容易多了 ——
　　　　　　　　现在只要测连接，就能反推位置，大大降低了研究难度。

Author contributions

M.P. developed and performed the simulations. M.P. and B.Sz. derived the analytical results. M.P. and L.B. analysed the empirical data. All authors contributed to the conceptual design of the study and the writing of the manuscript. A.-L.B. was the lead writer of the manuscript.

四、现实应用：用工具分析真实网络（果蝇大脑）
论文没有停留在理论，而是用"元图"分析了真实的果蝇大脑连接组（对应图 4），证明工具的"实战价值"：

构建"受限元图"：只看"物理上重叠但没有突触连接的神经元"（排除已经连了的，只看物理约束导致的"不能连"）；

发现规律：物理上"挤得越厉害"的神经元（元图里度越高），突触数量越多（功能越重要）—— 这说明大脑里"功能核心的神经元"反而被更多其他神经元"物理包围"，这是传统模型没法发现的；

解决痛点：之前不知道大脑连接组的形成是"遗传决定"还是"物理约束决定"，现在元图能量化物理约束的影响，为后续研究提供了工具。

五、总结：这篇论文的"贡献"是什么？
对学科来说，这篇论文做了三件大事：

补全了传统网络科学的短板：第一次建立了"物理约束"的量化理论框架，让网络科学能分析"有体积、不能交叉"的真实网络；

提供了实用工具：元图不仅能预测物理网络的拥堵、起效阈值，还能反推节点位置，甚至分析大脑、血管这些复杂系统；

启发新研究方向：未来可以用这个框架研究"超材料怎么设计更结实""芯片里的晶体管怎么摆不拥挤""大脑连接组的物理约束到底有多大影响"。